American Mineralogist, Volume 77, pages 617–630, 1992

Mineral chemistry and thermobarometry of a southern Appalachian amphibolite with epidote + quartz symplectite

CHRISTOPHER I. CHALOKWU
Department of Geology, Auburn University, Auburn, Alabama 36849, U.S.A.
SCOTT M. KUEHNER
Department of Geological Sciences, University of Washington, Seattle, Washington 98195, U.S.A.

ABSTRACT

The Uchee belt of the southern Appalachian Piedmont, in west-central Georgia, is a Barrovian metamorphic facies-series terrane that is characterized by a steeper metamorphic gradient than the adjacent Inner Piedmont rocks in Alabama. As a result of bulk compositional differences, amphibolites from the Uchee belt developed high- and low-variance subsets of the assemblage calcium amphibole + plagioclase + quartz + epidote + titanite ± garnet ± magnetite ± ilmenite ± rutile ± calcite ± diopside ± biotite. Plagioclase compositions change from An_{24} to An_{88} as a result of continuous reactions during prograde (M1) metamorphism. Amphiboles from symplectic rocks are typically zoned from tschermakitic cores [Mg/(Mg + Fe) = 59–77] to actinolite rims [Mg/(Mg + Fe) = 80–90]. Symplectites of epidote + quartz commonly occur around plagioclase and amphibole in garnet-free high-variance rocks, suggesting that the symplectites may have formed after (M1) metamorphism by the reaction 0.43 An_{50} + 1.00 Di [Mg/(Mg + Fe) = 55] + 0.33 H_2O + 0.14 O_2 → 0.26 Mg-Hbl + 0.17 Ep (Ps_{21}) + 0.82 Qtz. Another reaction, 23.97 An_{50} + 0.28 Mg-Hbl + 4.70 Ep (Ps_{21}) + 1.3 H_2O → 20.24 An_{38} + 0.17 Tr + 7.11 Ep (Ps_{15}) + 1.00 Qtz + 0.86 O_2, describes the mantling of amphibole by symplectite, the zoning in plagioclase to albitic compositions, zoning in amphibole to tremolite, and the depletion of Fe in symplectite epidote.

Thermobarometric studies indicate a maximum pressure of 10 ± 1 kbar and a temperature of 750 ± 30 °C for the prograde (M1) metamorphism followed by retrograde (M2) metamorphism at ~524 ± 50 °C and 6 kbar recorded by the symplectites. Modeling of symplectite-producing reactions suggests that the stable assemblage at upper amphibolite facies conditions was clinopyroxene + hornblende + plagioclase, which gave way to epidote symplectite and tremolite at lower amphibolite or upper greenschist facies conditions. The low equilibration temperature for symplectite, which is supported by low-pressure estimates calculated from reaction relationships, suggests that the symplectite formed during erosion and uplift along a path of low dP/dT immediately following the maximum P-T conditions. The composition of fluids during metamorphism of the Uchee belt, estimated from devolatilization equilibria, suggests the fluids were heterogeneous during (M1) metamorphism but were dominantly H_2O rich during retrograde (M2) metamorphism. The textural and compositional characteristics of retrograded amphibolites suggest that H_2O-rich fluids were important during progress of the symplectite-producing reactions.

INTRODUCTION

The Uchee belt is the complexly deformed southernmost exposed part of the Appalachian orogen and is of considerable importance in unraveling tectonic processes in the region. Recent interpretations by Hooper and Hatcher (1990) and Chalokwu and Hanley (1990) suggest that parts of the Uchee belt are relicts of an early Paleozoic back-arc basin accreted to the Laurentian continental margin and may have implications for the Piedmont-Avalon suture. Although field and structural studies have previously been interpreted in terms of emplacement of disparate tectonic domains or terranes, accompanied by ductile faulting and metamorphism (e.g., Bentley and Neathery, 1970; Glover et al., 1983; Hanley and Redwine, 1986; Hooper and Hatcher, 1990), no attempt has been made to characterize the conditions of metamorphism in this area. The Uchee belt in west-central Georgia and eastern Alabama is a Barrovian metamorphic terrane, characterized by an east-west transition from epidote amphibolite to amphibolite facies assemblages (Chalokwu, 1989). In addition to amphibolites, the western Uchee belt in Georgia consists of metasedimentary rocks, calc-silicates, migmatite, and granitic to monzonitic gneiss.

The purpose of this paper is to present results from the only detailed study of the compositional variations among

0003–004X/92/0506–0617$02.00

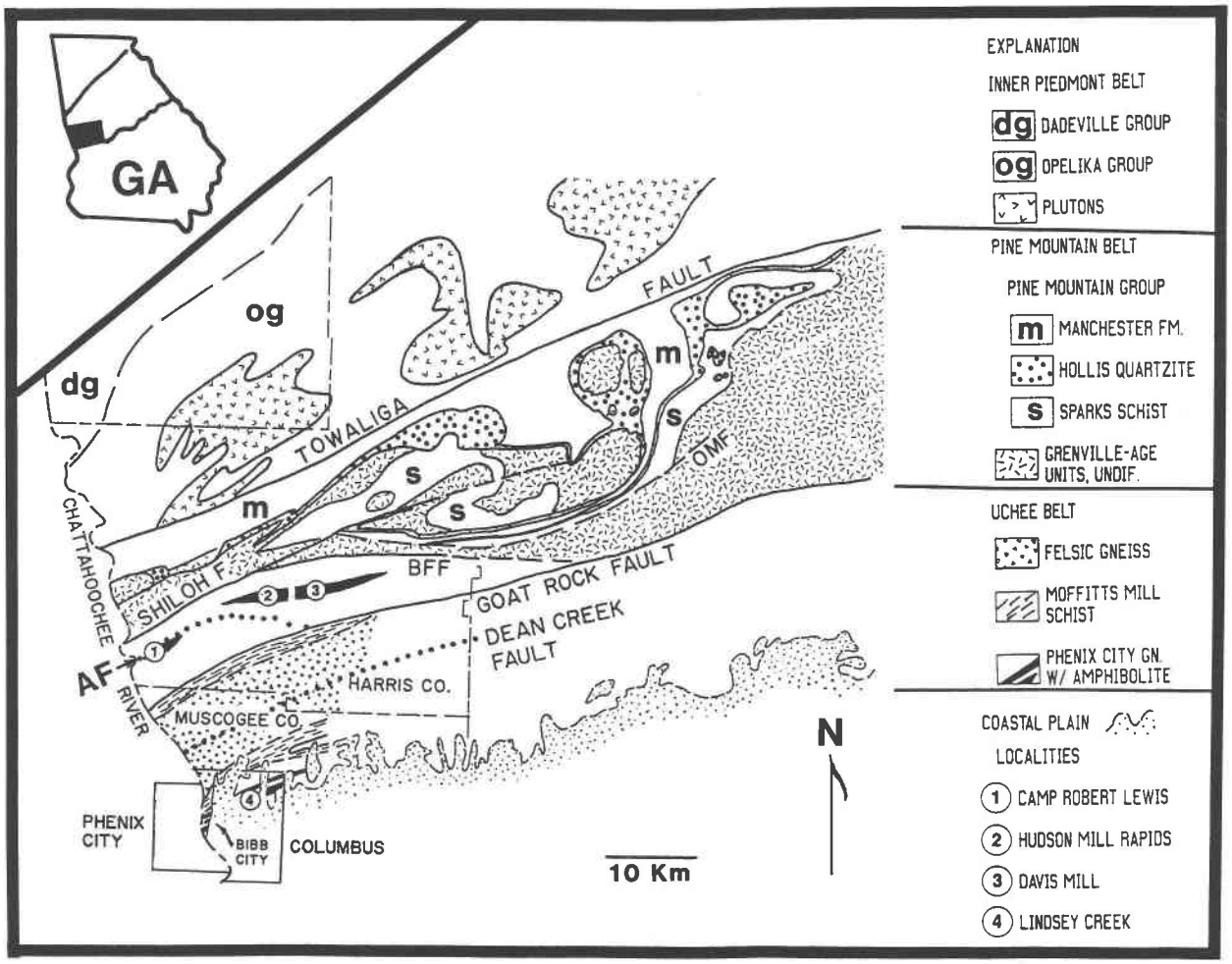

Fig. 1. Generalized geologic map of the west-central Georgia portion of the Uchee belt showing amphibolite localities and rocks of the adjacent Pine Mountain belt and Inner Piedmont (modified from Chalokwu and Hanley, 1990). OMF = Oak Mountain fault, BFF = Bartletts Ferry fault, AF = Auchumpkee fault.

minerals in Uchee belt amphibolites and to determine the metamorphic conditions using geothermometry and geobarometry. These data allow us to check for the internal consistency of several commonly applied thermometers and barometers and the evaluation of the most recently described plagioclase-hornblende thermometer (Blundy and Holland, 1990) and the garnet-plagioclase-hornblende-quartz barometer (Kohn and Spear, 1990). We also calculate the composition of fluids attendant during prograde (M1) and retrograde (M2) metamorphism of the Uchee belt from the temperature and pressure estimates. In a future study on kyanite- or sillimanite-bearing pelitic rocks intercalated with the amphibolites (Hanley and Redwine, 1986), we will present *P-T* data from which we will deduce the tectonic evolution of metamorphism in the southernmost exposed Appalachians.

Geologic setting

Bentley and Neathery (1970) described the Uchee belt as consisting of a sequence of amphibolite, amphibolitic gneiss, gneissic calc-silicate, and mylonitic rocks. Those authors considered the Goat Rock fault as the northern boundary of the Uchee belt (Fig. 1). However, recent studies suggest that a group of amphibolites and gneiss lying between the Bartletts Ferry fault (BFF) and Goat Rock fault are distinct from the Pine Mountain belt rock types and have been interpreted as a sliver of the Uchee belt (see Chalokwu and Hanley, 1990, and references therein). North of the Uchee belt is the Pine Mountain belt, which consists of Grenville basement rocks metamorphosed under granulite facies conditions (Sears and Cook, 1984). North of the Pine Mountain belt is the Inner Piedmont, much of which is in the sillimanite zone, with subordinate amounts of kyanite-bearing rocks (Glover et al., 1983). In the nearby Tallapoosa block of the northern Alabama Piedmont, metamorphism was largely in the kyanite zone (Gibson and Speer, 1986) and corresponded to lower temperature conditions compared with the adjacent Pine Mountain belt.

The timing of metamorphism in the southernmost Ap-

TABLE 1. Mineral assemblages in amphibolites

	Cam	Pl	Grt	Qtz	Ep	Cpx	Bt	Mag	Ilm	Ttn	Rt	Cal	Ap	Others
Hudson Mill Rapids														
HRA-1	X	X		X	X			X		X	X		X	
HRA-3	X	X	X	X	X_i		X	X		X			X	Scp
HRA-4	X	X		X	X		X_i	X						
HRA-5	X	X	X	X	X			X	X_i	X_i	X_i		X_i	sulfides, Scp
HRA-7	X	X	X_i	X	X			X	X	X	X_i			Sym
HRA-8	X	X	X	X	X			X	X	X	X			
HRA-9	X	X	X	X	X			X	X	X				
HRA-10	X	X	X	X	X				X	X	X			
HRA-16	X	X	X	X	X			X	X	X	X		X	sulfides
Davis Mill														
DMA-1	X	X		X	X			X		X				Chl*
DMA-1X	X	X	X	X	X	X		X_i	X	X	X			
DMA-2	X	X	X	X	X				X	X	X			
DMA-3	X	X		X	X		X			X	X			Sym
DMA-4	X	X		X	X	X	X	X		X	X	X		
DMA-5	X	X		X			X			X		X	X	Kfs
DMA-6	X	X		X	X			X		X		X		Kfs, Sym
DMA-11	X	X	X_i	X	X			X	X	X	X	X		Hem,* Sym
DMA-12	X	X		X	X	X		X		X	X	X		Sym
DMA-13	X	X		X	X		X			X	X	X		Chl,* Sym
Lindsey Creek														
LC-1	X	X		X	X	X		X	X	X	X	X		Scp
LC-2	X	X		X	X	X	X	X	X	X	X	X		Scp

Note: X_i = present as inclusions. Mineral abbreviations: Cam = calcium amphibole, Pl = plagioclase, Grt = garnet, Ep = epidote, Cpx = clinopyroxene, Scp = scapolite, Bt = biotite, Mg = magnetite, Ilm = ilmenite, Ttn = titanite, Rt = rutile, Cal = calcite, Ap = apatite, Hem = hematite, Chl = chlorite, Kfs = potassium feldspar, Sym = symplectic intergrowths of epidote + quartz. Sulfides are mostly pyrite and pyrrhotite.

* Present as alteration products.

palachians is poorly understood. An Acadian or Taconian age is generally assumed for (M1) metamorphism of this area, based on the occurrence of unmetamorphosed Carboniferous granitic plutons (e.g., Glover et al., 1983; Gibson and Speer, 1986). The faults that frame the Pine Mountain belt (including the Bartletts Ferry fault, which marks the northern boundary of the Uchee Belt; Fig. 1) have been interpreted by Hooper and Hatcher (1990) to be of mid-Paleozoic (Devonian) age. Recent ^{40}Ar-^{39}Ar cooling ages on hornblende from Uchee belt amphibolites and mylonites from the Goat Rock fault zone, however, suggest that the western Uchee belt in Georgia experienced amphibolite facies metamorphism and deformation during the late Carboniferous (Alleghanian) (Steltenpohl et al., 1990).

Three major amphibolites (Davis Mill, Hudson Mill Rapids, and Lindsey Creek), which were derived from basaltic protoliths (Chalokwu and Hanley, 1990), occur in the west-central Uchee belt in Georgia. Chalokwu (1989) recognized a garnet isograd that was the result of discontinuous reactions between biotite and epidote that produced hornblende and garnet. Also recognized at Lindsey Creek is the diopside isograd in amphibolites slightly high in bulk-rock Ca (12–14.4 wt%) compared with Davis Mill and Hudson Mill Rapids amphibolites (8–12.8 wt%; Chalokwu and Hanley, 1990). The slightly calcic rocks consist of subsets of the low-variance assemblage plagioclase + epidote + diopside + tremolite + quartz ± grossular ± calcite ± scapolite ± titanite ± ilmenite. The metamorphic grade varies from upper amphibolite facies to retrograde epidote-amphibolite facies.

ANALYTICAL TECHNIQUES

The mineral assemblage of each sample of amphibolite is presented in Table 1. Analyses of nonsymplectite mineral assemblages were obtained with a Kevex energy-dispersive spectrometer attached to a Cameca SX-50 electron microprobe at the University of Chicago. Analytical conditions were 15-kV, 10-nA Faraday cup current, and 60-s counting time. Anhydrous minerals and glasses were used for calibration. Symplectite mineral assemblages were analyzed using wavelength spectrometry with a four-spectrometer JEOL 733 Superprobe at the University of Washington. Analytical conditions of 15 kV, 20 nA were used with up to 40-s peak and background counting times. Possible alkali mobility in amphiboles and feldspars was reduced by counting K and Na X-rays first. Natural amphiboles and anhydrous minerals and glasses were used as standards and did not show any evidence of alkali mobility using the above procedure. We believe this procedure also minimizes the error in the estimation of ^{M4}Na in amphibole and the propagation of this error in amphibole-based thermometry.

Amphibole unit-cell formulae were obtained following the method of Robinson et al. (1982) by assuming initially that all Fe is FeO and then calculating Fe^{3+} from a charge balance based on 13 cations exclusive of Ca^{2+}, Na^+, and K^+ (hereafter referred to as the 13ECNK procedure). This method results in Fe^{3+} values that are intermediate between those based on normalization to 15 cations excluding Na and K (15ENK procedure) and normalization to 15 cations excluding K (15EK procedure).

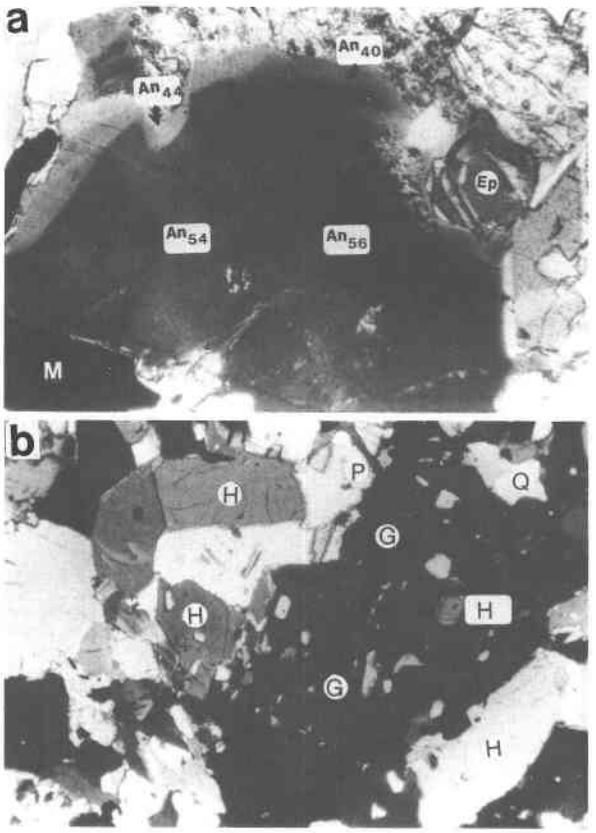

Fig. 2. Photomicrographs showing textural relationships in amphibolites. (**a**) Zoned and embayed plagioclase adjacent to epidote (Ep) and magnetite (M) in sample LC-1 from Lindsey Creek locality. Short dimension of field is approximately 0.9 mm. Crossed-polarized light. (**b**) Poikiloblastic garnet (G) with inclusions of quartz (Q) and amphibole (H) in sample HRA-10 from Hudson Mill Rapids. Matrix minerals include amphibole (H) and plagioclase (P). Short dimension of field is 1.08 mm. Cross-polarized light.

The exception is actinolite, for which the 13ECNK procedure resulted in unrealistically low (or negative) values of Fe^{3+}. We recalculated actinolite formulae by adopting the 15EK procedure, which forces all Na into the M4 site and results in intermediate values for Fe^{3+}. We also recalculated amphibole compositions using the average Fe^{3+} option of Spear and Kimball (1984), as required in the analytical plagioclase-hornblende thermometry of Blundy and Holland (1990). Recalculation of epidote compositions is based on the assumption that all Fe is Fe_2O_3. Other mineral compositions were recalculated assuming Fe_{tot} as FeO.

Petrography and mineral chemical relations

Plagioclase

Plagioclase is an important phase in all the samples studied. It occurs as anhedral to equigranular grains (Fig. 2) and as inclusions in garnet or amphibole. Plagioclase grains may also be partially to completely engulfed by symplectite consisting of epidote + quartz. Plagioclase is strongly zoned optically, especially where the plagioclase is next to epidote (Fig. 2a). Representative plagioclase analyses are given in Table 2.[1] The compositions of plagioclase range from oligoclase (An_{27}) at Davis Mill to bytownite (An_{88}) at Hudson Mill Rapids. The more common compositions are in the range An_{42-55} and An_{75-88} (Table 2).

Amphiboles

Representative compositions of amphiboles from both high- and low-variance assemblages are presented in Table 3. The amphiboles vary from blue-green to dark brown, depending upon grade, and are typically present in approximately 2:1 proportion with respect to plagioclase. According to the classifications of Leake (1978), the amphiboles are ferrotschermakite at Lindsey Creek and tschermakite at Hudson Mill Rapids and range in composition from tschermakite through magnesiohornblende to actinolite at Davis Mill. Although individual amphibole grains are rarely optically zoned, compositional zoning is present in symplectic rocks (e.g., sample DMA-12; Fig. 3) as determined from microprobe analysis and backscattered electron imaging (BEI). The zoning in sample DMA-12 ranges in composition from tschermakitic amphibole cores [Mg/(Mg + Fe) = 59–77] to actinolite rims [Mg/(Mg + Fe) = 80–90], with intermediate magnesiohornblende compositions located between the core and the rim (Fig. 3; Table 4). Al in amphibole is variable in symplectite domains but uniform in symplectite-absent rocks. The variability of Al in amphibole from the symplectite-rich domains (Table 4) is consistent with a hornblende-actinolite gap or disequilibrium, as suggested by Maruyama et al. (1983) for amphiboles from metabasites from Japan.

In order to understand the chemical trends in the amphiboles, plots of major amphibole substitutions were analyzed (Fig. 4). On a plot of $^{[4]}Al$ vs. A site, the amphiboles show substitution along the edenite vector ($Na^{[4]}AlSi_{-1}$) and cluster in a field that is intermediate between tschermakite and pargasite end-members (Fig. 4a). The variation between $^{[4]}Al$ and $^{[6]}Al$ (Fig. 4b) also indicates a strong deviation in amphibole compositions from an ideal tschermakite-like ($^{[4]}Al^{[6]}AlMg_{-1}Si_{-1}$) substitution vector of slope 1 to lines with slopes of 2 and above. Both tschermakite ($^{[4]}Al^{[6]}AlMg_{-1}Si_{-1}$) and edenite ($Na^{[4]}AlSi_{-1}$) substitutions occur, so that there is more $^{[4]}Al$ than that ascribed to tschermakite alone. Similarly, the sum of cations involving a Tschermak-like coupled substitution (Fig. 4c) correlates poorly with a line of slope 1. The correlation between $^{[4]}Al$ and the sum of the cations involved in increasing $^{[4]}Al$ (by Tschermak and edenite

[1] To obtain a copy of Tables 2, 3, and 5, order Document AM-92-497 from the Business Office, Mineralogical Society of America, 1130 Seventeenth Street NW, Suite 330, Washington, DC 20036, U.S.A. Please remit $5.00 in advance for the microfiche.

TABLE 4. Representative compositions of amphibole and the anorthite content of associated plagioclase from symplectite-rich domains of rock DMA-12

Domain	4	5	6	6	6	6
Spot	Cam1	Cam1	Cam4	Cam5	Cam6	Cam7
SiO_2	44.69	43.67	43.29	44.49	55.02	46.16
TiO_2	0.74	0.66	0.62	0.61	0.05	0.54
Al_2O_3	11.89	11.42	11.93	11.73	1.50	9.60
FeO	13.56	15.39	15.83	11.51	5.22	13.78
MnO	0.31	0.27	0.22	0.33	0.23	0.30
MgO	11.96	11.34	10.75	13.47	19.49	12.61
CaO	12.55	12.29	12.06	12.49	14.05	12.17
Na_2O	1.21	1.38	1.40	1.29	0.10	1.03
K_2O	0.76	0.78	0.86	0.80	0.03	0.55
Total	97.67	97.20	96.96	96.72	95.69	96.74
			Cations per 23 O atoms*			
Si	6.557	6.489	6.465	6.516	7.809	6.803
$^{[4]}Al$	1.443	1.511	1.535	1.484	0.191	1.197
$^{[6]}Al$	0.613	0.489	0.566	0.542	0.060	0.471
Fe^{3+}	0.209	0.376	0.337	0.372	0.142	0.293
Ti	0.082	0.074	0.069	0.067	0.005	0.060
Mg	2.615	2.511	2.392	2.940	4.123	2.770
Fe^{2+}	1.455	1.536	1.641	1.038	0.478	1.406
Mn	0.039	0.034	0.028	0.041	0.028	0.037
Ca	1.973	1.957	1.930	1.960	1.972	1.922
$^{[M4]}Na$	0.014	0.023	0.038	0.040	0.028	0.042
$^{[A]}Na$	0.330	0.374	0.368	0.326	0.000	0.252
K	0.142	0.148	0.164	0.149	0.005	0.103
A site	0.472	0.522	0.532	0.476	0.005	0.355
Pl(An)	0.34	0.41	0.38	0.38	0.40	0.40
T_S	402	495	510	494	NC	512
T_{BH}	730	767	762	751	NC	697

Note: Cam = calcium amphibole. Numbers in parentheses for domains 6 and 4 correspond to spot analyses in Figures 3a and 3b, respectively. T_S = Plagioclase-hornblende temperatures (°C) using calibration of Spear (1980). T_{BH} = Plagioclase-hornblende temperatures using Blundy and Holland (1990) analytical thermometer calculated for a reference P of 7 kbar. NC = not calculated; amphibole composition outside the recommended range for the analytical plagioclase-hornblende thermometer. Details of the temperature calculations are presented later in the section on thermobarometry.

* Amphibole composition calculated for average Fe^{3+} using the program Recamp (Spear and Kimball, 1984).

substitutions) has a slope that is somewhat less than 1 (Fig. 4d), indicating a glaucophane-type ($^{[M4]}Na^{[6]}Al$ = CaMg) or plagioclase-type ($^{[M4]}NaSi$ = $Ca^{[4]}Al$) substitution in the amphibole compositions. Ti-tschermakite substitution is not indicated for these amphiboles because Ti varies widely for any given $^{[4]}Al$ (Fig. 4e).

Garnet

Garnet is an important phase in the low-variance rocks with the subassemblage garnet + hornblende + plagioclase + quartz ± epidote. It occurs as relatively large (3–6 mm) anhedral to subrounded poikiloblastic grains with inclusions of quartz (Fig. 2b), plagioclase, hornblende, and, rarely, epidote and apatite. Garnet is absent in the symplectite-bearing rocks, with the exception of samples DMA-11 and HRA-7, where it is present as inclusions in amphibole. This suggests that garnet, if present, is now absent from symplectic rocks because it was consumed by reactions producing the corona textures. The ranges of the garnet components are 50–63 mol% almandine, 7–17 mol% pyrope, 2–18 mol% spessartine, and 18–28 mol% grossular (Table 5). Most garnets are strongly chemically zoned from calcic cores to Mn-rich rims, accompanied by only a slight core to rim increase in the Mg/(Mg + Fe) ratio.

Epidote

Epidote from low-variance assemblages occurs as highly birefringent, rounded to equant, randomly scattered grains that are typically zoned both optically and compositionally. Epidote from the high-variance assemblage calcium amphibole + quartz + epidote + plagioclase + titanite occurs as inclusions in amphibole and as the dominant phase in epidote + quartz symplectite-rich domains (Fig. 3).

Representative analyses of epidote are presented in Table 6. The epidote is restricted in composition to pistacite (Ps) contents (100 $Fe^{3+}/(Fe^{3+} + Al)$] of 15–27, compared with epidote from mafic schists from other areas (e.g., Vermont),which generally contain widely varying amounts of Ps (12–70 mol%; Laird and Albee, 1981; Spear, 1982). Fe in epidote decreases with increasing metamorphic grade. The absence of zoisite indicates relatively high metamorphic temperatures for the amphibolites (Maruyama et al., 1983). Epidote in symplectite is generally Fe poor (e.g., 5.8–11.8 wt% Fe_{tot} as Fe_2O_3), compared with epidote in nonsymplectic rocks (9.7–14 wt% Fe_2O_3). Moody et al. (1983) concluded from experimental studies of mafic systems that the composition of epidote is a function of P and T as well as of the bulk-rock composition.

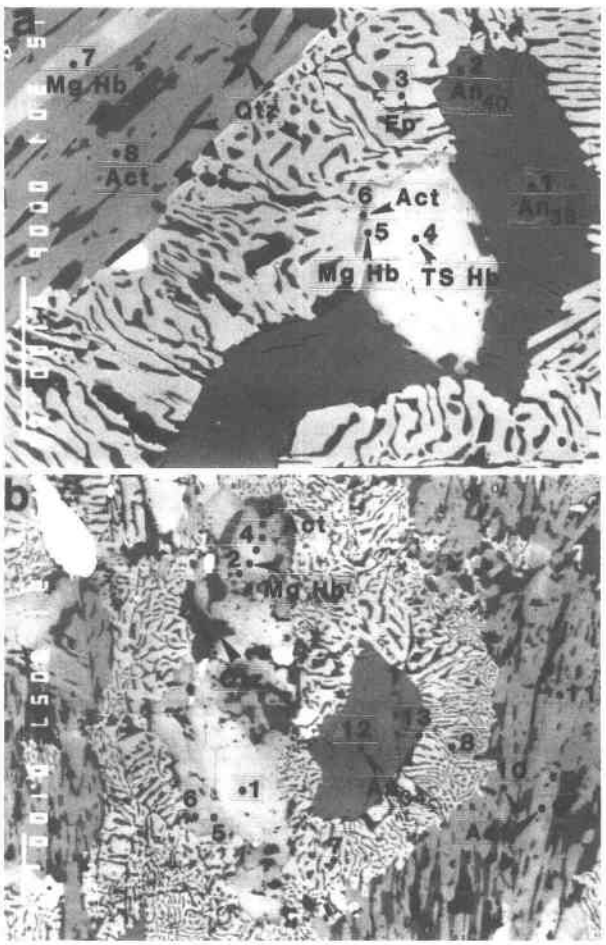

Fig. 3. Backscattered electron images (BEI) of symplectite from symplectite-rich domains in sample DMA-12 from Davis Mill. (**a**) Epidote + quartz symplectite partially enclosing plagioclase (An_{38-40}) and zoned amphibole from domain 6. Note amphibole at center is zoned from tschermakitic hornblende core to actinolite rim. Also note actinolite at upper left of field with inclusions of quartz and relict magnesiohornblende. Amphibole and plagioclase compositions corresponding to numbered spot analyses are given in Table 4. Abbreviations: Act = actinolite; Mg Hb = magnesiohornblende; TS Hb = tschermakitic hornblende; Ep = epidote; Qtz = quartz (scale bar = 100 μm). (**b**) BEI of symplectite from domain 4 of sample DMA-12. Abbreviations as in **a**. Note the separation of actinolite from plagioclase by symplectite, which is the common mode of occurrence in most domains (cf. **a**) (scale bar = 100 μm).

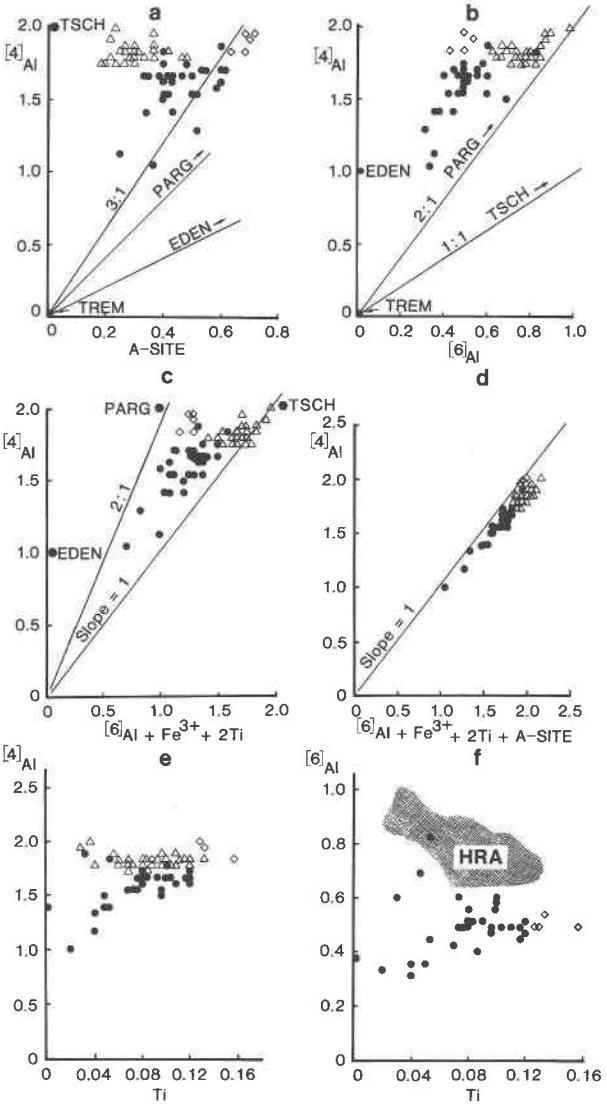

Fig. 4. Variation of amphibole compositions (solid circles = Davis Mill samples, triangles = Hudson Mill Rapids, and diamonds = Lindsey Creek. End-member abbreviations: PARG = pargasite; EDEN = edenite; TSCH = tschermakite; TREM = tremolite). (**a**) Plot of $^{[4]}$Al vs. A site [$^{[A]}$(Na + K)]. (**b**) Plot of $^{[4]}$Al vs. $^{[6]}$Al illustrating deviation of amphibole compositions from a line of slope 1 indicating a tschermakite substitution vector. (**c**) Plot of $^{[4]}$Al vs. $^{[6]}$Al + Fe^{3+} + 2Ti showing M2-site substitution. (**d**) Plot of $^{[4]}$Al vs. $^{[6]}$Al + Fe^{3+} + 2Ti + A site illustrating the effect of A-site substitution. (**e**) Plot of $^{[4]}$Al vs. Ti showing uniform $^{[4]}$Al for Hudson Mill Rapids and Lindsey Creek relative to Davis Mill amphibolites. (**f**) Plot of $^{[6]}$Al vs. Ti showing a general inverse relationship for Hudson Mill Rapids (ruled field, HRA) but not for Davis Mill amphibolites.

Clinopyroxenes

The composition of clinopyroxenes ranges in X_{Mg} [Mg/(Mg + Fe)] from ~0.5 to 0.8 (Table 6). Clinopyroxenes are modally subordinate (<1 vol%) or absent in the symplectic rocks but are relatively abundant in rocks from Lindsey Creek (up to 10 vol%). The presence of absence of clinopyroxene in Uchee belt amphibolites is thought to be primarily a function of P and T and bulk-rock chemistry; i.e., only rocks with bulk CaO from 11 to 14.4 wt% contain clinopyroxene (see Chalokwu and Hanley, 1990).

Minor phases

Additional minor phases include scapolite, with Ca/(Ca + Na) from 0.73 to 0.78, and calcite, with only trace amounts of Fe (<0.3 wt%). Titanite was not subjected to

Table 6. Representative microprobe analyses of epidote and clinopyroxene

	HRA-4	HRA-8	HRA-9	DMA-1X	DMA-1	DMA-4	DMA-12*	DMA-13*	LC-2	DMA-1X	DMA-4	DMA-12	LC-1	LC-2
					Epidote							Clinopyroxene		
SiO_2	38.39	38.20	38.50	37.86	38.16	38.08	39.27	38.35	38.03	51.53	51.54	56.22	50.26	48.61
Al_2O_3	24.92	24.61	24.12	25.59	25.53	24.57	27.06	24.64	23.12	1.19	1.08	1.49	2.45	3.95
Fe_2O_3**	11.23	11.04	11.93	9.89	10.30	11.60	7.63	11.80	13.09	10.13	9.88	7.45	13.56	13.86
MnO	0.20	0.42	0.31	0.19	0.22	0.21	0.15	0.29	0.25	0.46	0.36	0.22	0.58	0.63
MgO	0.00	0.00	0.00	0.00	0.00	0.00	0.18	0.00	0.00	12.13	12.93	19.78	9.20	8.74
TiO_2	0.00	0.10	0.15	0.21	0.14	0.00	0.00	0.12	0.24	0.16	0.11	0.01	0.25	0.33
CaO	23.76	23.18	23.20	23.70	23.77	23.65	23.81	23.28	23.70	23.61	23.81	13.29	23.35	23.14
Na_2O	n.d.	n.d.	n.d.	n.d.	n.d.	n.d.	n.d.	n.d.	n.d.	0.52	0.46	0.31	0.81	0.73
K_2O	0.00	0.06	0.00	0.05	0.05	0.08	0.07	0.05	0.05	0.05	0.04	0.00	0.04	0.00
Total	98.50	97.57	98.21	97.49	98.17	98.19	98.17	98.53	98.48	99.78	100.23	98.77	100.50	99.99
					Cations per 12.5 O atoms							Cations per six O atoms		
Si	3.015	3.026	3.037	2.994	2.999	3.007	3.049	3.015	3.014	1.955	1.945	2.037	1.925	1.877
Al	2.309	2.300	2.244	2.388	2.368	2.289	2.479	2.825	2.162	0.053	0.048	0.063	0.111	0.180
Fe	0.664	0.659	0.709	0.589	0.610	0.690	0.446	0.699	0.781	0.321	0.312	0.226	0.434	0.448
Mn	0.013	0.028	0.021	0.013	0.015	0.014	0.010	0.019	0.017	0.015	0.012	0.006	0.019	0.021
Mg	0.000	0.000	0.000	0.000	0.000	0.000	0.021	0.000	0.000	0.686	0.727	1.068	0.525	0.503
Ti	0.000	0.006	0.009	0.013	0.008	0.000	0.000	0.007	0.014	0.005	0.003	0.000	0.007	0.009
Ca	1.999	1.968	1.961	2.009	2.003	2.002	1.982	1.961	2.013	0.960	0.963	0.516	0.959	0.958
Na	—	—	—	—	—	—	—	—	—	0.038	0.034	0.022	0.060	0.055
K	0.000	0.006	0.000	0.005	0.005	0.008	0.007	0.005	0.005	0.002	0.002	0.000	0.002	0.000
Sum	8.000	7.993	7.981	8.011	8.008	8.010	7.994	7.991	8.006	4.035	4.046	3.938	4.042	4.051
X_{ps}	0.22	0.22	0.24	0.20	0.21	0.23	0.15	0.23	0.27	X_{mg} 0.681	0.700	0.825	0.547	0.529
a_{Czo}	0.35	0.37	0.31	0.43	0.41	0.33	0.58	0.31	0.24					

Note: n.d. = not determined.
* Epidote from symplectic rocks.
** Total Fe as Fe_2O_3 for epidote and as FeO for clinopyroxene.

electron microprobe analysis. Biotite, when present, occurs in trace amounts principally along amphibole grain boundaries and rarely as rims on epidote from nonsymplectite domains.

Mineral reactions and reaction textures

The composition of plagioclase rims from a nonsymplectite rock from Lindsey Creek (sample LC-1) appears to be dependent upon the adjacent epidote. For example, the plagioclase rim (An_{40}) adjacent to an epidote crystal with a reaction halo in sample LC-1 (Fig. 2a) is more albitic than the core (An_{56}), suggesting that the epidote formed at the expense of plagioclase by a net transfer reaction such as 14 Ab + 4 H_2O = Tr + 6 Czo + 5 Tk ($Al_2Mg_{-1}Si_{-1}$) + 14 $NaSiCa_{-1}Al_{-1}$ + 7 Qtz. Also, Uchee belt amphibolites that contain garnet generally have little or no biotite, suggesting the isograd discontinuous reaction proposed by Abbott (1982) for metabasites:

$$\text{epidote} + \text{biotite} \rightarrow \text{hornblende} + \text{garnet}. \quad (1)$$

Alternatively, the rarity of biotite and chlorite may be due to the net transfer reaction:

$$\text{plagioclase} + \text{chlorite} + \text{biotite} \rightarrow \text{hornblende} + \text{garnet}. \quad (2)$$

A detailed study of symplectite-rich domains in amphibolite was greatly facilitated using BEI (Fig. 3). By this imaging technique, chemical zoning within individual grains could be visually resolved. Approximately 50 microprobe analyses of calcium amphibole, plagioclase, and epidote were obtained from six symplectite-rich domains in sample DMA-12, with representative compositions of Cam and the anorthite content of associated Pl presented in Table 4. The symplectite consists of rims and mantles of fine-grained epidote + quartz intergrowths (in approximately 2.6:1 volume proportion) separating amphibole and plagioclase or completely enclosing embayed plagioclase and amphibole (Fig. 3b). Amphiboles, whether adjacent to symplectite or engulfed by it, are usually zoned from tschermakitic or magnesiohornblende cores to magnesiohornblende or actinolite rims adjacent to the symplectite, and they also contain numerous quartz lamellae.

Curiously, plagioclase and amphibole are rarely in contact near the symplectite-rich domains, even though both phases are seemingly in textural equilibrium, throughout the remainder of a given section. This observation, coupled with the presence of numerous quartz lamellae in the symplectite-associated amphibole (Fig. 3a), suggests that the symplectite did not form by reaction between quartz-bearing amphibole and plagioclase. In contrast, these features imply that the quartz-bearing amphibole is a product instead of a reactant. The formation of symplectite may be represented by the generalized reaction

$$5\ \text{Di} + 9\ \text{An} + 4\ H_2O \rightarrow 6\ \text{Czo} + \text{Tr} + 2\ \text{Qtz}. \quad (3a)$$

Using plagioclase (An_{50}) and epidote (Ps_{21}) compositions from symplectite-free portions of sample DMA-12, symplectite amphibole from Table 4 (analysis Cam4, Fig. 3a) and diopside composition from unaltered sample LC-1 (Table 6), mass balance calculations yield

$$0.43\ An_{50} + 1.00\ \text{Di}\ [\text{Mg}/(\text{Mg} + \text{Fe}) = 55] + 0.33\ H_2O + 0.14\ O_2 \rightarrow 0.25\ \text{Mg-Hbl} + 0.17\ \text{Ep}\ (Ps_{21}) + 0.82\ \text{Qtz}. \quad (3b)$$

The calculation describes the formation of magnesiohornblende and epidote + quartz symplectite and sup-

TABLE 7. Thermobarometry and mineral composition of Uchee belt amphobolites

Sample	Garnet				Amphibole		Plag	Grt-Hb	
	X_{Alm}	X_{Prp}	X_{Sps}	X_{Grs}	X_{Mg}	X_{Fe}	X_{An}	T_{GP}	T_{PET}
HRA-5	0.567	0.164	0.045	0.224	1.986	1.834	0.394	738	684
	0.586	0.165	0.037	0.212	1.982	2.012	0.351	699	632
HRA-8	0.595	0.120	0.092	0.194(r)	1.783	2.318(c)	0.581	662	633
	0.581	0.131	0.075	0.213(r)	1.783	2.324(r)	0.581	706	662
HRA-9	0.590	0.129	0.104	0.177(r)	1.950	2.244(r)	0.83	636	630
	0.581	0.106	0.105	0.207(c)	1.870	2.205(c)	0.80	625	588
HRA-1					1.715	1.748	0.475	—	—
HRA-4					2.115	1.548	0.748	—	—
HRA-7					1.920	1.721	0.860	—	—
HRA-10	0.598	0.173	0.050	0.179	1.849	2.394	0.645	745	731
HRA-16	0.575	0.157	0.045	0.223	1.886	2.343	0.805	758	703
DMA-1X	0.495	0.094	0.028	0.383	2.109	2.483	0.362	750	596
DMA-2	0.500	0.088	0.129	0.283	1.736	2.384	0.357	718	615
DMA-11	0.512	0.109	0.118	0.262	2.092	2.297	0.280	690	606
DMA-12‖					3.760	1.041(r)	0.409(r)	—	—

Note: Abbreviations for barometer: GPHQ = garnet-plagioclase-hornblende-quartz; GPHEQ = garnet-plagioclase-hornblende-epidote-quartz; GPCQ = garnet-plagioclase-clinopyroxene-quartz; GRIPS = garnet-rutile-ilmenite-plagioclase-silica (Qtz). Subscripts for *T* and *P*: GP = Graham and Powell (1984), PET = Perchuk et al. (1985), S = Spear (1980), KS = Kohn and Spear (1990), W = Wells (1979), BH = Blundy and Holland (1990), NP = Newton and Perkins (1982), BL = Bohlen and Liotta (1986), HS = Hodges and Spear (1982). P_{RCT} = pressure deduced from reactions. Ref = Reference *P* for analytical Pl-Hb thermometer, r = rim, c = core.

* Average pressure estimated from two or more barometers.

** P_{Ref} assumed.

† Pressure deduced from epidote breakdown reaction curve (Apted and Liou, 1983).

‡ Pressure estimated from the reaction An = CaTs + Qtz (Ellis, 1980).

§ Pressure estimated from Reactions 3a and 7 calculated from Ge0-Calc (Berman et al., 1987) using actual mineral compositions.

‖ See Table 4 for more *T* estimates for sample DMA-12.

ports our petrographic observation that diopside occurs in trace amounts (or is totally consumed) in symplectic rocks. The calculation also indicates that the production of epidote + quartz symplectite and of amphibole with numerous quartz lamellae should be favored if a_{H_2O} is high and the reaction is sufficiently oxidizing. Chalokwu (1989) estimated an f_{O_2} that was 2 log units above the QFM buffer (at 540 °C) for sample LC-2 from Lindsey Creek. This, and the presence of Fe-Ti oxides in the symplectic rocks, suggests that an oxidation reaction such as Reaction 3b has indeed taken place. In order to account for the relict magnesiohornblende in actinolitic amphibole (Table 4, analysis Cam7; Fig. 3a) and the albite-rich plagioclase and Fe-poor epidote associated with the symplectites, another reaction was calculated:

$$23.97\ An_{50} + 0.28\ \text{Mg-Hbl} + 4.70\ Ep\ (Ps_{21}) + 1.3\ H_2O \rightarrow 20.24\ An_{38} + 0.17\ Tr + 7.11\ Ep\ (Ps_{15}) + 1.00\ Qtz + 0.86\ O_2. \quad (4)$$

With the exception of plagioclase (An_{50}) and epidote (Ps_{21}) which are from nonsymplectite portions of sample DMA-12, all mineral compositions used for calculating Reaction 4 are from symplectites (Table 4; Fig. 3). The resulting assemblage is consistent with the observed depletion of Fe in epidote (perhaps by Fe = Al exchange), with the zoning in amphibole to tremolite, and with the decrease in plagioclase mode near symplectite (e.g., Fig. 3b).

The rarity of garnet in symplectic rocks (i.e., garnet is present as inclusions in amphibole in samples DMA-11 and HRA-7), the decrease in modal titanite, and the occurrence of ilmenite with symplectite suggest that these phases may have been involved in the following generalized reactions:

$$2\ Rt + Ttn + Alm \rightarrow An + 3\ Ilm + 2\ Qtz \quad (5)$$

and

$$8\ Alm + \text{Fe-Chl} + 10\ Rt + 14\ Ttn \rightarrow 6\ Czo + Act + 24\ Ilm + 15\ Qtz. \quad (6)$$

Reaction 6 is supported by the observations that chlorite occurs as alteration and rutile as inclusions in titanite (Table 1) and that amphibole becomes more actinolitic near symplectite-rich regions (Fig. 3a). Later in this paper we model Reaction 3a and other reactions to provide additional constraints on the metamorphic *P-T* evolution of the amphibolites.

THERMOBAROMETRY

The changes in mineral compositions of amphibolites from the Uchee belt, southern Appalachian Piedmont, have been interpreted to reflect a transition from epidote amphibolite to the amphibolite facies conditions (Chalokwu, 1989). As a result of bulk compositional differences (Chalokwu and Hanley, 1990), the amphibolites developed diverse mineral assemblages that are suitable for quantitative thermobarometry. Two sets of temperatures and pressures have been determined for these rocks; temperatures and pressures during (M1) metamorphism and during the later retrograde event (M2). A retrograde *P-T* path is constructed based on the presence of reaction textures.

TABLE 7—*Continued*

Pl-Hb			GPHQ	GPHEQ	GPCQ		GRIPS	
T_S	T_{BH}	P_{Ref}	P_{KS}	P_W	P_{NP}	P_{HS}	P_{BL}	P_{RCT}
645	740	9.6*	9.5				9.7	
725	712	10**	8.8	—	—	—	9.2	
560	849	9.3**	7.5	—	—	—	—	
578	828	9.8**	7.2	—	—	—	—	
525	865	7.6**	6.5	—	—	—	—	
550	856	7.4*	7.2	7.5	—	—	—	
516	842	10**						4.7†
523	803	11**						5†
524	804	11**						5*
725	838	9.8**	7.4	—	—	—	—	
570	786	10.0*	9.2	11	—	—	9.4	
507	634	10*	10.7	—	10.2	9.3	11.5	9‡
530	723	12**	9.4	—	—	—	9.8	
520	652	13**	10.2	—	—	—	—	
524	526							5.5,† 4.6–5§

Temperature

Temperature estimates are based largely on the garnet-hornblende and plagioclase-hornblende thermometers (Table 7). Application of garnet-hornblende Fe-Mg exchange thermometry, following the calibration of Graham and Powell (1984), yielded temperatures ranging from 625 to 758 ± 30 °C. Temperatures obtained within any single thin section from the nonsymplectic rocks, using the rim compositions of garnet and hornblende (Tables 5, 7), are similar to estimates made with the core compositions (Table 7). We interpret this to mean that the nonsymplectic amphibolites are reasonably well equilibrated and that they have not experienced significant Fe-Mg reequilibration during cooling, as has been described by Tracy (1982). Application of the Perchuk et al. (1985) calibration of the garnet-hornblende thermometer yielded temperatures of 6–84 °C less than those obtained from the Graham and Powell (1984) calibration, with the exception of samples DMA-1X and DMA-2 (Table 7). We prefer the Graham and Powell (1984) calibration because it nicely reproduces temperatures within a single thin section, using several combinations of mineral compositions. Application of the garnet-clinopyroxene thermometer (Ellis and Green, 1979) to sample DMA-1X using an estimated pressure of 9 ± 2 kbar yields a temperature of 725 ± 30 °C, consistent with the garnet-hornblende temperature (750 ± 30 °C; Graham and Powell, 1984).

Unlike the garnet-hornblende thermometer, which could not be applied to all of the amphibolites, the plagioclase-hornblende thermometer may be used with all samples. Indeed, in some high-variance rocks such as DMA-1 and DMA-12, the plagioclase-hornblende thermometer is the only applicable thermometer (Tables 4, 7). The thermometer was first calibrated by Spear (1980) as a graphical thermometer based upon the exchange NaSi = CaAl. Application of the plagioclase-hornblende thermometer is complicated by uncertainties in the estimation of the amount of Fe^{3+} and hence of the amount of ^{M4}Na in amphibole. The graphical plagioclase-hornblende thermometer yields temperatures of 402–725 °C, which in many instances compare poorly with the Graham and Powell (1984) or the Perchuk et al. (1985) garnet-hornblende temperatures (Tables 4, 7).

We have also compared the temperatures derived from the semiempirical plagioclase-hornblende thermometer of Blundy and Holland (1990) with temperatures obtained from the graphical thermometer of Spear (1980). Temperatures obtained with the Blundy and Holland thermometer range from 526 to 865 °C (at P_{Ref} of 6–13 kbar), which in some cases are up to 340 °C higher than estimates made using the graphical thermometer of Spear, and 50–235 °C higher than the garnet-hornblende temperatures (Tables 4, 7). Blundy and Holland (1990) obtained similarly high temperatures when the thermometer was applied to amphibolites from Vermont. They attributed the discrepancy to lack of equilibrium, plagioclase unmixing, and to nonideality. The analyzed mineral compositions from the Uchee belt amphibolites meet the compositional restrictions imposed in the calibration (e.g., plagioclase < An_{92} and amphibole < 7.8 atoms of Si per formula unit). We therefore suggest that the cause of the high temperatures determined with this thermometer has to do with inappropriate mineral assemblages or calibration problems.

A point not sufficiently addressed in the description of uncertainties associated with the plagioclase-hornblende thermometer (Blundy and Holland, 1990, p. 218) is the effect of assumed or calculated pressure on the estimated temperatures. If, as we have concluded, the garnet-hornblende thermometer provides the best estimate of maximum temperature of metamorphism for the amphibolites, an unreasonably high pressure of 15 kbar would be required for temperatures obtained from the Blundy and Holland (1990) thermometer to conform with garnet-hornblende temperatures. We estimate that the effect of pressure on the temperatures with this thermometer is about 18 °C/kbar, which, when combined with the other error terms described by Blundy and Holland (1990), could raise the overall uncertainties in the thermometer

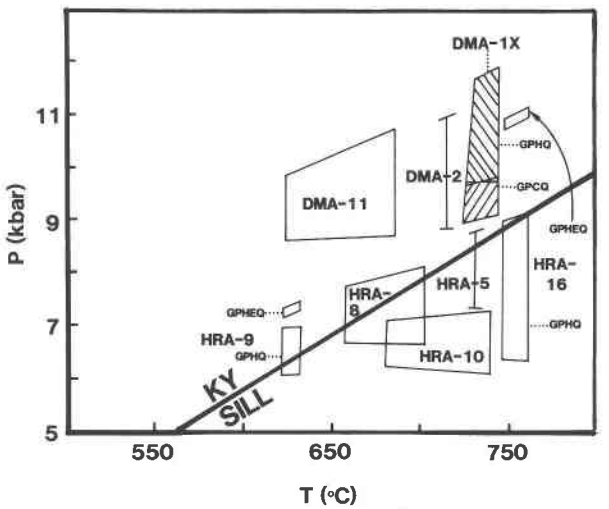

Fig. 5. Selected *P-T* data for Uchee belt amphibolites from simultaneous solution of the garnet-hornblende thermometer (Graham and Powell, 1984) and the garnet-plagioclase-hornblende-quartz barometer (GPHQ; Kohn and Spear, 1990), the garnet-plagioclase-hornblende-epidote-quartz barometer (GPHEQ; Wells, 1979) and the garnet-plagioclase-clinopyroxene-quartz barometer (GPCQ; Newton and Perkins, 1982). Kyanite-sillimanite (KY-SILL) equilibrium after Holdaway (1971) is shown for reference. In general Davis Mill amphibolites (with DMA prefix) reflect higher pressures of equilibration than do Hudson Mill Rapids amphibolites (HRA) or Lindsey Creek amphibolites (not shown).

to ±90 °C. In contrast, the effect of pressure on temperature using the garnet-clinopyroxene thermometer, which also requires an estimated pressure in order to obtain a temperature, is only 2 °C/kbar (Ellis and Green, 1979).

Pressure

Amphibolites from the Uchee belt lack critical index minerals (e.g., orthoamphibole, kyanite, staurolite, etc.) from which metamorphic pressures could be readily deduced using published petrogenetic grids (e.g., Spear and Rumble, 1986). We estimated pressures directly using the following fluid-independent barometers: garnet-plagioclase-hornblende-quartz (GPHQ; Kohn and Spear, 1990; P_{KS}), garnet-plagioclase-hornblende-epidote-quartz (GPHEQ; Wells, 1979; P_W), garnet-plagioclase-clinopyroxene-quartz (GPCQ; Newton and Perkins, 1982; P_{NP}; and Hodges and Spear, 1982; P_{HS}), and garnet-rutile-ilmenite-plagioclase-quartz (GRIPS; Bohlen and Liotta, 1986; P_{BL}). Results of the calculations are presented in Table 7 and Figure 5.

The barometer best suited for amphibolites from the Uchee belt is the GPHQ barometer (Kohn and Spear, 1990). Application of the GPHQ barometer using maximum temperatures from the Graham and Powell (1984) garnet-hornblende thermometer yields pressures from 6.5 ± 1 kbar at the Hudson Mill Rapids locality to 10.7 ± 1 kbar at Davis Mill. It is instructive to compare GPHQ pressures with pressures from well-tested barometers such as GRIPS, since both were calibrated for garnet amphibolites and have similar precision (±500 and ±300 bars for GPHQ and GRIPS, respectively). Application of the GRIPS barometer to four samples (HRA-5, HRA-16, DMA-1X, and DMA-2) results in pressures that are indistinguishable from those derived from GPHQ barometer (Table 7).

The GPHEQ barometer (Wells, 1979) is of limited application to Uchee belt amphibolites because most epidote-bearing rocks are devoid of garnet. The difficulty encountered with the GPHEQ barometer is determining what constitutes an equilibrium epidote composition, especially for the symplectic rocks for which the mere presence of symplectite implies disequilibrium. Two nonsymplectic samples (HRA-9 and HRA-16) were evaluated for consistency between GPHQ and GPHEQ barometers. Although pressures obtained using the two barometers are almost identical for sample HRA-9 (7.2 and 7.5 kbar), the calculated pressures differ significantly for sample HRA-16 (9.2 and 11 kbar; Fig. 5). In general, for a given temperature the GPHEQ barometer places sample HRA-16 in the kyanite field, whereas the GPHQ barometer places sample HRA-16 in the sillimanite stability field. A similar disparity was noted by Hudson (1985), who applied the GPHEQ barometer to Buchan rocks of the Scottish Dalradian.

Sample DMA-1X is the only sample (out of 30) with the proper low-variance assemblage (calcium amphibole + plagioclase + garnet + epidote + clinopyroxene + quartz + magnetite + ilmenite + titanite + rutile) that can be used to check for internal consistency of the two barometers (GPHQ and GPCQ; Tables 6, 7) described above and the barometer based on the reaction An = CaTs + Qtz (Ellis, 1980). The agreement between these barometers for sample DMA-1X is quite striking (9.3–10.7 kbar; average = 9.8 ± 0.6 kbar). We therefore conclude that the best estimate of maximum pressure recorded in sample DMA-1X, and the highest pressure of metamorphism for the Uchee belt, is ~10 kbar at 750 °C.

Metamorphic fluid composition

Several equilibria can be used to estimate fluid compositions during prograde (M1) and retrograde (M2) metamorphism of the Uchee belt, including Reaction 3a, which we interpret to be responsible for the formation of the symplectites. Activity-composition relations for minerals used to calculate fluid compositions are presented in Table 8. Table 9 lists the equilibria (Reactions 7–16) that buffer fluid activities determined using the method described by Perkins et al. (1986) and Berman et al. (1987). In some case, two devolatilization equilibria were evaluated for a sample, depending upon mineral assemblage, to check for internal consistency of the estimated fluid compositions. The compositions of metamorphic fluid were calculated using the Fortran program Ge0-Calc (Perkins et al., 1986; Berman et al., 1987) and *P-T* data

TABLE 8. Calculation of mole fractions and activity models of end-member components in minerals

Mole fraction	
Garnet	
X_{Prp}	= Mg/(Mg + Fe + Mn + Ca)
X_{Grs}	= Ca/(Mg + Fe + Mn + Ca)
X_{Alm}	= Fe/(Mg + Fe + Mn + Ca)
X_{Sps}	= Mn/(Mg + Fe + Mn + Ca)
Plagioclase	
X_{An}	= Ca/(Ca + Na + K)
Activity	
a_{An}	$= Y_{An}X_{An}(1 + X_{An}^2)/4$ (Al avoidance model; Newton et al., 1980)
a_{Alm}^{Grt}	$= \{X_{Alm}\exp[(13800 - 6.28T)(-X_{Prp}X_{Grs})/RT]\}^3$ (Hodges and Spear, 1982)
a_{Tr}	= (3 − Ca − Na − K)(Ca/2)²(Mg/5)⁵ (coupled susbitution model; Ghent, 1988)
a_{Tr}	$= (X_{O,A})(X_{Ca,M4})^2(X_{Mg,M13})^5[X_{Si,T_1}]^4$ (ideal mixing on sites; Blundy and Holland, 1990)
a_{Czo}^{Ep}	$= X_{Al,M3}^{Ep}$ or (Ca/2)²(1 − [Fe³⁺ + Mn])(Si/3)³
a_{Di}^{Cpx}	= (Ca)(Mg)(Si/2)²

given in Table 7 (mostly garnet-hornblende temperatures and GPHQ pressures). Actual mineral compositions (Tables 2–6) were used to calculate activity coefficients, except for ilmenite, magnetite, titanite, and, in some cases, diopside, for which ideal compositions were assumed.

Although we tested several activity models for garnet, including the simple pyrope-almandine regular solution model, the quaternary garnet mixing model of Hodges and Spear (1982) is preferred because it produces more internally consistent results for garnet-dependent equilibria than other garnet activity models and because some of the temperature and pressure estimates (Table 7) were also based on this model. The activity of tremolite is based on ideal crystalline solution models (Ghent, 1988). Solution of the equilibria in Table 9 utilizes a nonideal H_2O-CO_2 mixing model and a modified Redlich-Kwong equation of state (Kerrick and Jacobs, 1981).

Although it was not possible to quantify the errors in these calculations, the equilibria used for calculating fluid compositions are known to be sensitive to P, T, and the activity models adopted. Thus the a_{H_2O} values obtained should be considered only approximate. We have a better understanding of the effect of pressure and temperature on the calculated fluid compositions than we do for the effect of the activity models. For example, symplectic amphibolite sample DMA-12 lacks the critical assemblage for estimating metamorphic pressure from geobarometry. For this sample, pressures of 4.6–6.0 ± 2 kbar for the formation of the symplectite were estimated using a reaction limiting the stability of epidote (Apted and Liou, 1983) and Ge0-Calc software (Perkins et al., 1986; Berman et al., 1987) to calculate Reactions 3a and 7 with actual mineral compositions (Tables 4, 6) and estimated a_{H_2O}. We applied a sensitivity test to the calculated fluid compositions in lieu of a rigorous error analysis that incorporates all sources of errors in a single error estimation. For symplectic sample DMA-12, an error of ±50 °C from plagioclase-hornblende thermometry changes the a_{H_2O} by +0.11 and −0.03, and an error of ±2 kbar pressure affects calculated a_{H_2O} by ±0.28.

A T-a_{CO_2} diagram is presented in Figure 6 for mineral assemblages that buffer fluid compositions during a retrograde event (M2), exemplified by symplectic samples DMA-12 and HRA-7. The thin section of sample DMA-12 contains fine-grained calcite, which appears to have equilibrated texturally with epidote + plagioclase + titanite + quartz. The subassemblage anorthite + calcite + epidote is shown to be stable in H_2O-rich fluids over a wide range of temperature (Fig. 6), from which maximum a_{CO_2} at 6 kbar is constrained to 0.24 ± 0.02, based on Reaction 13. Reactions 8, 10, and 13 intersect near 500 °C and near a_{CO_2} = 0.07 at 6 kbar (Fig. 6). This is interpreted to represent the minimum a_{CO_2} during symplectite formation. The low a_{CO_2} (0.07–0.24 ± 0.02) is consistent with mass balance calculations that indicate that H_2O was an important fluid phase during progress of the symplectite-producing reaction (Reaction 4).

TABLE 9. Summary of a_{H_2O} and related equilibria

Sample	a_{Alm}	a_{An}	a_{Czo}	a_{Tr}	a_{Di}	T	P	(a_{H_2O}) (3a)	(a_{H_2O}) (7)	(a_{H_2O}) (8)	(a_{H_2O}) (10)	(a_{H_2O}) (11)	(a_{H_2O}) (12)	(a_{H_2O}) (13)	(a_{H_2O}) (14)	(a_{H_2O}) (15)
HRA-5	0.19	0.86	0.38*	0.05	—	699	9	—	—	—	—	0.45	—	—	—	—
HRA-7	0.16**	0.94	0.43	0.006	—	524	5	—	0.73	0.71	—	—	—	—	—	0.66
HRA-9	0.19	0.86	0.31	0.005	—	636	7	—	—	—	—	—	—	—	0.88	0.82
HRA-16	0.18	0.96	0.38	0.003	—	758	9.5	—	—	—	—	—	—	—	0.82	0.82
DMA-1X	0.11	0.80	0.43	0.008	0.63	750	10.0	>0.65	—	—	—	—	0.57	—	—	—
DMA-12	—	0.66	0.58	0.025	0.66	524	6	0.75	—	—	0.87	—	—	0.76	—	—
LC-1	—	0.69	0.24	0.001	0.46	634†	7.2	—	—	—	0.32	—	—	<0.50	—	—

Reactions

6 Czo + Tr + 2 Qtz = 5 Di + 9 An + 4 H_2O (3a)
3 Ilm + 4 Qtz + 4 Czo = 3 Ttn + 5 An + Alm + 2 H_2O (7)
Qtz + Rt + 2 Czo = Ttn + 3 An + H_2O (8)
3 Ttn + Tr = 3 Rt + Qtz + 5 Di + H_2O (9)
Rt + Qtz + Cal = Ttn + CO_2 (10)
CO_2 + Czo = Me + H_2O (11)
2 Ttn + Tr + 2 Czo = 2 Rt + 5 Di + 3 An + 2 H_2O (12)
CO_2 + 2 Czo = 3 An + Cal + H_2O (13)
Alm + 4 Rt + 4 Czo = 7 An + 3 Ilm + Ttn + 2 H_2O (14)
Alm + 3 Rt + 2 Czo = 4 An + 3 Ilm + Qtz + H_2O (15)
Cal + 2 Ttn + Tr = 5 Di + 2 Rt + CO_2 + H_2O (16)

Note: Samples HRA-7 and DMA-12 contain simplectites and were used to constrain the composition of the retrograde (M2) fluids.
* Activity of Czo assumed.
** Activity of Alm assumed.
† T estimated from plagioclase-scapolite thermometry (Chalokwu, 1989).

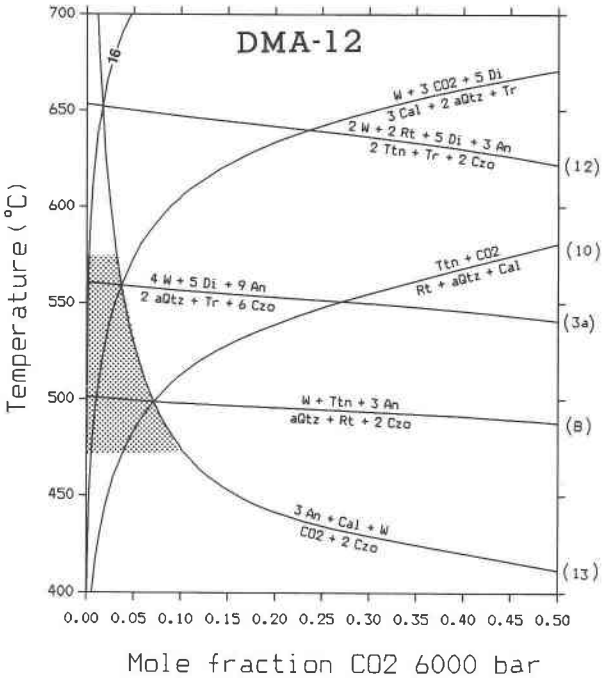

Fig. 6. T-X_{CO_2} diagram at 6 kbar for symplectic amphibolite DMA-12 showing the H_2O-rich nature of fluids (stippled) present during retrograde (M2) metamorphism. The stippled area is based on an uncertainty of ±50 °C in plagioclase-hornblende temperature. Mineral abbreviations after Kretz (1983); aQtz = α quartz. Reaction 16 is Cal + 2 Ttn + Tr = 5 Di + 2 Rt + CO_2 + H_2O.

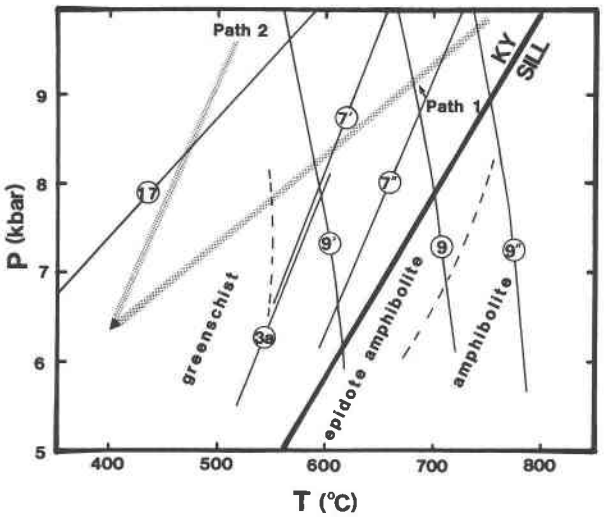

Fig. 7. P-T diagram for symplectite-forming reactions compared with other equilibria. Reaction boundaries computed using GeO-Calc (Berman et al., 1987), observed mineral compositions (Tables 4, 6), and activity models given in Table 8. Isopleth for Reaction 3a was computed using measured compositions of plagioclase, amphibole, and epidote (Tables 4, 6) and a = 1.0 for diopside and quartz. Isopleths for Reaction 7 were calculated for Fe-poor (Reaction 7′) and Fe-rich (Reaction 7″) compositions of epidote, for plagioclase (An_{34-41}; Table 4), and for a = 1.0 for Ilm, Qtz, Ttn, and Alm. Reaction 9 is plotted using a = 1.0 for all minerals; Reactions 9′ and 9″ correspond to Reaction 9 plotted for a range of mineral compositions (Table 4; Figs. 3a, 3b). The isopleth for Reaction 17, Ep + Rt + Di + Alm = An + Ilm + Qtz + Tr, was calculated using a = 1.0 for all minerals. Also shown for comparison are greenschist, epidote amphibolite, and amphibolite facies boundaries (Apted and Liou, 1983; Moody et al., 1983) and, for reference, the kyanite-sillimanite (KY-SILL) equilibrium (Holdaway, 1971). Inferred P-T paths discussed in the text (1 and 2) are shown as dotted stripes.

An estimate of metamorphic fluid composition during prograde (M1) metamorphism can be made based on the occurrence of titanite vs. rutile (± titanite, ± ilmenite). Rutile is either absent or occurs as inclusions in garnet, amphibole, and titanite (e.g., samples HRA-5, HRA-7, and HRA-9). The fluid buffering reaction (Reaction 14), applied to samples HRA-9 and HRA-16 at P = 7.0 and 9.3 kbar and T = 636 and 758 °C, yields a_{H_2O} of 0.88 and 0.82, respectively, for the prograde (M1) metamorphism. These values contrast with the range of a_{H_2O} calculated for the same assemblage from samples DMA-1X (0.57–0.65) and LC-1 (0.32–<0.50), suggesting that the fluids were compositionally heterogeneous throughout the Uchee belt during prograde metamorphism of the amphibolites. A similar conclusion was obtained from an examination of prograde metamorphic assemblages in pelitic schists from the nearby Inner Piedmont of Alabama (Chalokwu and Colberg, 1990).

Discussion

Several studies of amphibolite and granulite facies terranes have emphasized the importance of near-isobaric cooling or near-isothermal decompression paths in the formation of symplectic textures (e.g., de Wit and Strong, 1975; Harley, 1989). Harley (1989) presented criteria for recognizing these paths in granulite terranes, where symplectite textures are more readily preserved than in amphibolites because granulites are metamorphosed at higher temperature and pressure. Symplectic amphibolites from the Uchee belt are used to provide additional constraints on metamorphic conditions and the retrograde P-T paths followed by the amphibolites. As a working hypothesis, we infer that the symplectites developed during retrograde segments of a P-T evolution. The absence of high-pressure assemblages with orthopyroxene and the rarity of garnet from symplectic rocks of the Uchee belt relative to granulites complicates the task of differentiating isothermal decompression from isobaric cooling paths but precludes symplectite formation due to compression or with heating.

Reaction modeling for symplectic amphibolite DMA-12 is compared with experimental greenschist-amphibolite transition equilibria in Figure 7 to test the hypothesis for symplectite formation. The dP/dT slopes for Reactions 3a, 7, 9, and 17 were modeled for observed mineral

compositions (Tables 4, 6) using activity models presented in Table 8 and for assumed mineral compositions with unit activity (e.g., ilmenite, titanite, rutile, quartz). A thermodynamic argument can be made for a near-isobaric cooling path (or possibly increasing P with decreasing T) if it can be shown that symplectite-producing reactions (Reactions 3a, 7) have shallow or zero dP/dT slopes such that a strong temperature dependency was involved. Calculations indicate that the formation of Czo + Tr + Qtz at the expense of Pl + Di + H_2O (Reaction 3a) is a pressure-dependent reaction with a dP/dT slope of 30 bars/°C. Reaction 17 has a shallower slope (13 bars/°C). Also, Reaction 7 has slopes of 26–28 bars/°C for a range of tabulated mineral compositions (Table 4), which compares quite favorably with the dP/dT slope of 28.5 bars/°C for the reaction Ep + Qtz = Grt + An + Mt + fluid, determined experimentally by Liou (1973, p. 403).

The absence of garnet and clinopyroxene in most symplectic rocks of the Uchee belt (Table 1) implies that garnet may have been involved in discontinuous reactions at high pressures and that clinopyroxene is stable only at high pressures when the temperature is greater than 650 °C, according to Reaction 9 (Fig. 7). Reaction 9 produces nonsymplectic end-members (i.e., all symplectites contain epidote), and its steep dP/dT slope of −83 bars/°C indicates a strong pressure instead of temperature dependence. Consequently, we can eliminate a near-isothermal decompression path that is subparallel to the univariant equilibrium 3 Ttn + Tr = 3 Rt + Qtz + 5 Di + H_2O (Reaction 9) because such a path is associated with minor heating with decompression instead of minor cooling, as described by Harley (1989, p. 230) for granulites.

The P-T path that is considered most likely for the amphibolites (path 1, Fig. 7) is one that crosses Reactions 3a and 7 from the maximum T of metamorphism (~750 °C) to the final temperatures of 402–526 ± 50 °C recorded by symplectites. This interpretation is consistent with the requirement that the symplectite assemblage forms on the low-temperature side of a reaction with small, positive dP/dT if near-isobaric cooling is to be a viable option.

Experimental studies by Moody et al. (1983) and Maruyama et al. (1983) indicate a lower temperature stability limit of ~500 °C for titanite in the presence of CO_2. The low equilibration temperatures recorded by the symplectites (404–526 °C) and the presence of titanite in symplectitic rocks from the Uchee belt are consistent with the above experimental results. It is also possible that the amphibolites followed a series of near-isothermal decompression paths that crossed Reaction 17 (e.g., path 2 in Fig. 7), or a series of paths that included near-isobaric cooling and near-isothermal decompression, as deduced by Chalokwu (1990) based on garnet zoning profiles and mineral inclusions in nonsymplectic rocks.

As a result of the P-T data presented here, we can infer the overburden thickness during metamorphism of the Uchee belt. Davis Mill amphibolites were more deeply buried or metamorphosed (up to 36 km) than Hudson Mill Rapids (30 km) and Lindsey Creek (20 km) counterparts and were buried even deeper than pelitic rocks from the neighboring Inner Piedmont in Alabama, which had an overburden thickness of ~28 km at the peak of metamorphism (Gibson and Speer, 1986; Chalokwu and Colberg, 1990). We conclude that amphibolites from the Uchee belt in west-central Georgia record the maximum thermal and baric conditions yet documented for metamorphism in the exposed southernmost Appalachians. The proximity of these rocks to granulite facies basement rocks in the Pine Mountain belt (e.g., Sears and Cook, 1984) is enigmatic and suggests that the Uchee belt amphibolites may skirt an amphibolite-granulite facies transition boundary in this area rather than occupy a separate and distinct tectonic feature, as thought by essentially all previous workers.

Acknowledgments

Acknowledgment is made to the donors of the Petroleum Research Fund, administered by the American Chemical Society, for financial support. Additional support was provided by NSF grant EAR-8817074 to C.I.C. Thanks are extended to D.M. Jenkins and M.J. Kohn for providing valuable discussions and to F.S. Spear for making available some of the computer programs used in this study. The manuscript has benefited from reviews by M.J. Kohn, R.N. Abbott, Jr., S.M. Swapp, and Jo Laird. Eva Lilly and Tracy Tatum painstakingly typed the tables.

References cited

Abbott, R.N., Jr. (1982) Petrogenetic grid for high-grade metabasites. American Mineralogist, 67, 865–876.

Apted, M.J., and Liou, J.G. (1983) Phase relations among greenschist, epidote-amphibolite, and amphibolite in a basaltic system. American Journal of Science, 283-A, 328–354.

Bentley, R.D., and Neathery, T.L. (1970) Geology of the Brevard fault zone and related rocks of the inner Piedmont of Alabama. Alabama Geological Society Field Trip Guidebook, 119 p. Alabama Geological Society, Auburn, Alabama.

Berman, R.G., Brown T.H., and Perkins, E.H. (1987) GeO-CALC: Software for calculation and display of pressure-temperature-composition phase diagrams. American Mineralogist, 72, 861–862.

Blundy, J.D., and Holland, T.J.B. (1990) Calcic amphibole equilibria and a new amphibole-plagioclase geothermometer. Contributions to Mineralogy and Petrology, 104, 208–224.

Bohlen, S.R., and Liotta, J.J. (1986) A barometer for garnet amphibolites and garnet granulites. Journal of Petrology, 27, 1025–1034.

Chalokwu, C.I. (1989) Epidote-amphibolite to amphibolite facies transition in the southern Appalachian Piedmont: P-T conditions across the garnet and calc-silicate isograds. Geology, 17, 491–494.

——— (1990) Metamorphic P-T paths and exhumation of the southernmost Appalachian Piedmont deduced from reaction textures and mineral zoning in amphibolites (abs.). International Geological Correlation Program Project 235: Metamorphic styles in young and ancient orogenic belts, p. 23. University of Calgary, Calgary.

Chalokwu, C.I., and Colberg, M. (1990) Thermobarometry and calculated fluid composition of migmatitic schists in the contact zone of the Farmville Granite, Alabama Piedmont. Geological Society of America Abstracts with Programs, 22, 258.

Chalokwu, C.I., and Hanley, T.B. (1990) Geochemistry, petrogenesis, and tectonic setting of amphibolites from the southernmost exposure of the Appalachian Piedmont. Journal of Geology, 98, 725–738.

de Wit, M.J., and Strong, D.F. (1975) Eclogite-baring amphibolites from the Appalachian mobile belt, northwest Newfoundland: Dry versus wet metamorphism. Journal of Geology, 83, 609–627.

Ellis, D.J. (1980) Osumilite-sapphirine-quartz granulite from Enderby Land, Antarctica: P-T conditions of metamorphism, implications for

garnet-cordierite equilibria and the evolution of the deep crust. Contributions to Mineralogy and Petrology, 74, 201–210.

Ellis, D.J., and Green, D.H. (1979) An experimental study of the effect of Ca upon garnet-clinopyroxene Fe-Mg exchange equilibria. Contributions to Mineralogy and Petrology, 71, 13–22.

Ghent, E.D. (1988) Tremolite and H_2O activity attending metamorphism of hornblende-plagioclase-garnet assemblages. Contributions to Mineralogy and Petrology, 98, 163–168.

Gibson, R.G., and Speer, J.A. (1986) Contact aureoles as constraints on regional P-T trajectories: An example from the northern Alabama Piedmont, USA. Journal of Metamorphic Geology, 4, 285–308.

Glover, L., III, Speer, J.A., Russell, G.S., and Farrar, S.S. (1983) Ages of metamorphism and ductile deformation in the central and southern Appalachians. Lithos, 16, 223–245.

Graham, C.M., and Powell, R. (1984) A garnet-hornblende geothermometer: Calibration, testing, and application to the Pelona Schist, southern California. Journal of Metamorphic Geology, 2, 13–31.

Hanley, T.B., and Redwine, J.C. (1986) The Bartletts Ferry and Goat Rock fault zones north of Columbus, Georgia. In T.L. Neathery, Ed., Southeastern section of the Geological Society of America: Centinnial field guide, vol. 6, p. 291–296. Geological Society of America, Denver.

Harley, S.L. (1989) The origins of granulites: A metamorphic perspective. Geological Magazine, 126 (3), 215–247.

Hodges, K.V., and Spear, F.S. (1982) Geothermometry, geobarometry and the Al_2SiO_5 triple point at Mt. Moosilauke, New Hampshire. American Mineralogist, 67, 1118–1134.

Holdaway, M.J. (1971) Stability of andalusite and the aluminosilicate phase diagram. American Journal of Science, 271, 97–131.

Hooper, R.J., and Hatcher, R.J., Jr. (1990) Ocmulgee fault: The Piedmont-Avalon terrane boundary in central Georgia. Geology, 18, 708–711.

Hudson, N.F.C. (1985) Conditions of Dalradian metamorphism in the Buchan area, NE Scotland. Journal of the Geological Society of London, 142, 63–76.

Kerrick, D.M., and Jacobs, G.K. (1981) A modified Redlich-Kwong equation for H_2O, CO_2, and H_2O-CO_2 mixtures at elevated pressures and temperatures. American Journal of Science, 281, 735–767.

Kohn, M.J., and Spear, F.S. (1990) Two new geobarometers for garnet amphibolites, with applications to southeastern Vermont. American Mineralogist, 75, 89–96.

Kretz, R. (1983) Symbols for rock-forming minerals. American Mineralogist, 68, 277–279.

Laird, J., and Albee, A.L. (1981) Pressure, temperature, and time indicators in mafic schist: Their application to reconstructing the polymetamorphic history of Vermont. American Journal of Science, 281, 127–175.

Leake, B.E. (1978) Nomenclature of amphiboles. Canadian Mineralogist, 16, 501–520.

Liou, J.G. (1973) Synthesis and stability relations of epidote, $Ca_2Al_2FeSi_3O_{12}(OH)$. Journal of Petrology, 14, 381–413.

Maruyama, S., Suzuki, K., and Liou, J.G. (1983) Greenschist-amphibolite transition equilibria at low pressures. Journal of Petrology, 24, 583–604.

Moody, J.B., Meyer, D., and Jenkins, J.E. (1983) Experimental characterization of the greenschist/amphibolite boundary in mafic systems. American Journal of Science, 283, 48–92.

Newton, R.C., and Perkins, D., III (1982) Thermodynamic calibration of geobarometers based on the assemblages garnet-plagioclase-orthopyroxene (clinopyroxene)-quartz. American Mineralogist, 67, 203–222.

Newton, R.C., Charlu, T.V., and Kleppa, O.J. (1980) Thermochemistry of the high structural state plagioclases. Geochimica et Cosmochimica Acta, 44, 933–941.

Perchuk, L.L., Aranovich, L.Y., Podlesskii, K.K., Lavrant'eva, I.V., Gerasimov, V.Y., Fed'Kin, V.V., Kitsul, V.I., Karasakov, L.P., and Berdnikov, N.V. (1985) Precambrian granulites of the Aldan shield, eastern Siberia, USSR. Journal of Metamorphic Geology, 3, 265–310.

Perkins, E.H., Brown, T.H., and Berman, R.G. (1986) PT-SYSTEM, TX-SYSTEM, PX-SYSTEM: Three programs which calculate pressure-temperature-composition phase diagrams. Computers and Geosciences, 12, 749–755.

Robinson, P., Spear, F.S., Schumacher, J.C., Laird, J., Klein, C., Evans, B.W., and Doolan, B.L. (1982) Phase relations of metamorphic amphiboles: Natural occurrences and theory. In Mineralogical Society of America Reviews in Mineralogy, 9B, 1–227.

Sears, J.W., and Cook, R.B., Jr. (1984) An overview of the Grenville basement complex of the Pine Mountain window, Alabama and Georgia. In M.J. Barthlomew, Ed., The Grenville event in the Appalachians and related topics. Geological Society of America Special Paper, 194, 281–287.

Spear, F.S. (1980) NaSi = CaAl exchange equilibrium between plagioclase and amphibole: An empirical model. Contributions to Mineralogy and Petrology, 72, 33–41.

——— (1982) Phase equilibria of amphibolites from the Post Pond Volcanics, Mt. Cube quadrangle, Vermont. Journal of Petrology, 23, 383–426.

Spear, F.S., and Kimball, C. (1984) RECAMP—a Fortran IV program for estimating Fe^{3+} contents of amphiboles. Computers & Geosciences, 10, 317–325.

Spear, F.S., and Rumble, D., III (1986) Pressure, temperature and structural evolution of the Orfordville belt, west-central New Hampshire. Journal of Petrology, 27, 1071–1093.

Steltenpohl, M.G., Goldberg, S.A., Kunk, M.J., and McRae, M., (1990) Structural and age relations from the Goat Rock fault zone, Alabama and Georgia: Evidence for Alleghanian development. Geological Society of America Abstracts, 22, 233.

Tracy, R.J. (1982) Compositional zoning and inclusion in metamorphic minerals. Mineralogical Society of America Reviews in Mineralogy, 10, 355–397.

Wells, P.R.A. (1979) P-T conditions in the Moines of the central highlands, Scotland. Geological Society of London Journal, 136, 663–671.

Manuscript received August 9, 1990
Manuscript accepted January 23, 1992